Deciphering deformation along submarine fault branches below the eastern Sea of Marmara (Turkey): Insights from seismicity, strainmeter, and GPS data

***Virginie Durand** (GFZ)*

A.Gualandi (INGV), P.Martínez-Garzón (GFZ), G.Kwiatek (GFZ), M.Haghighi (Leibniz Univ.), M.Motagh (GFZ), G.Dresen (GFZ, Univ.Potsdam) & M.Bohnhoff (GFZ, Free Univ. Berlin)

Context

Complex region where seismic and aseismic slip can interact

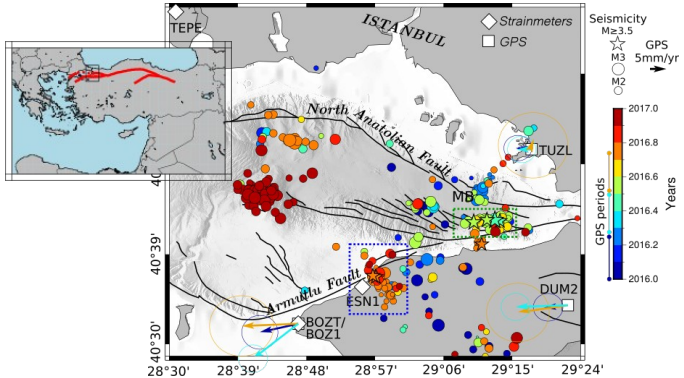

***Location map:** seismic activity during 2016, location of the GPS and strainmeter stations, GPS velocities averaged on 3month-periods from Jan. to Sep. 2016*

GPS data

A slow transient recorded at one GPS station in April 2016

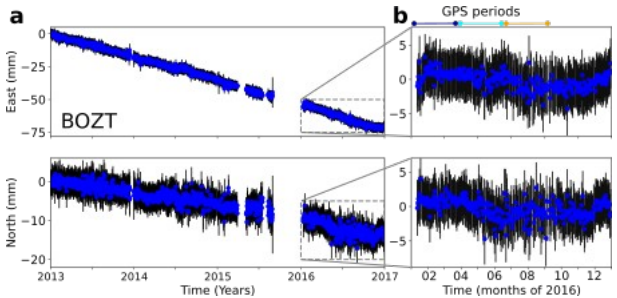

***GPS station BOZT:** a) Signal recorded between 2013 and 2017, corrected from seasonal variations. The slope represents the long-term trend (~18mm/year) b) Zoom on 2016, signal corrected from seasonal variations, long-term trend removed. (Processed signal : courtesy of S. Ergintav, KOERI)*

Strainmeter data - vbICA

Extraction of the seasonal component

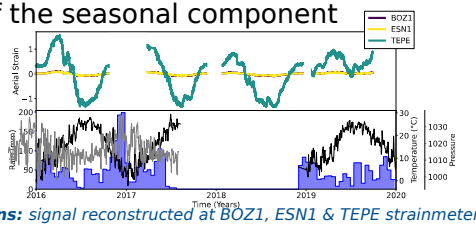

***Seasonal variations:** signal reconstructed at BOZ1, ESN1 & TEPE strainmeter stations using only the seasonal component. Comparison with meteorological data*

Integration of the different data

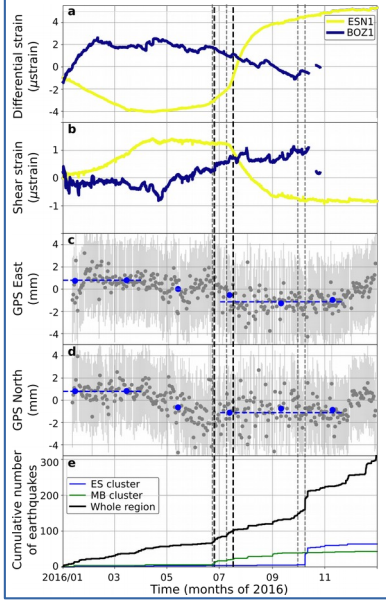

A 2-step transient is visible in the GPS and strainmeter data.

This transient is followed by an activation of the seismicity

***Comparison of the available data during 2016:** a) and b) Differential and shear strains recorded at BOZ1 and ESN1 stations. c) and d) East and North GPS components at BOZT station e) Temporal evolution of the seismicity on two clusters. The green curve corresponds to the seismicity in the green box on the Location Map, the blue curve to the one in the blue box, and the black curve to the seismicity in the whole region.*

Coulomb modelling

2 consecutive events on 2 perpendicular faults

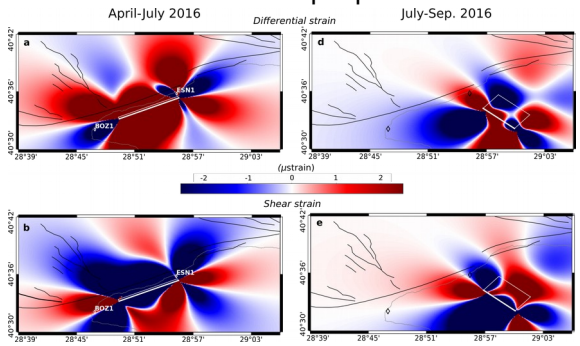

***Coulomb modelling of the 2 transients:** Left : 1st event, Right : 2nd event. Up : Differential strain, Down : shear strain*

Conclusions

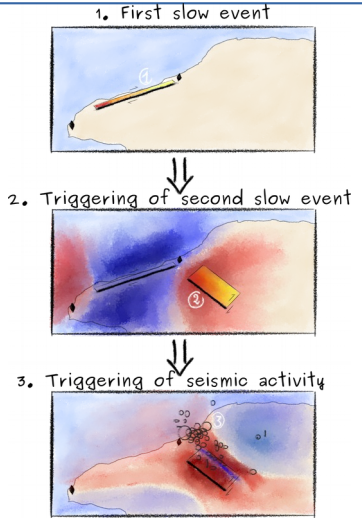

Context

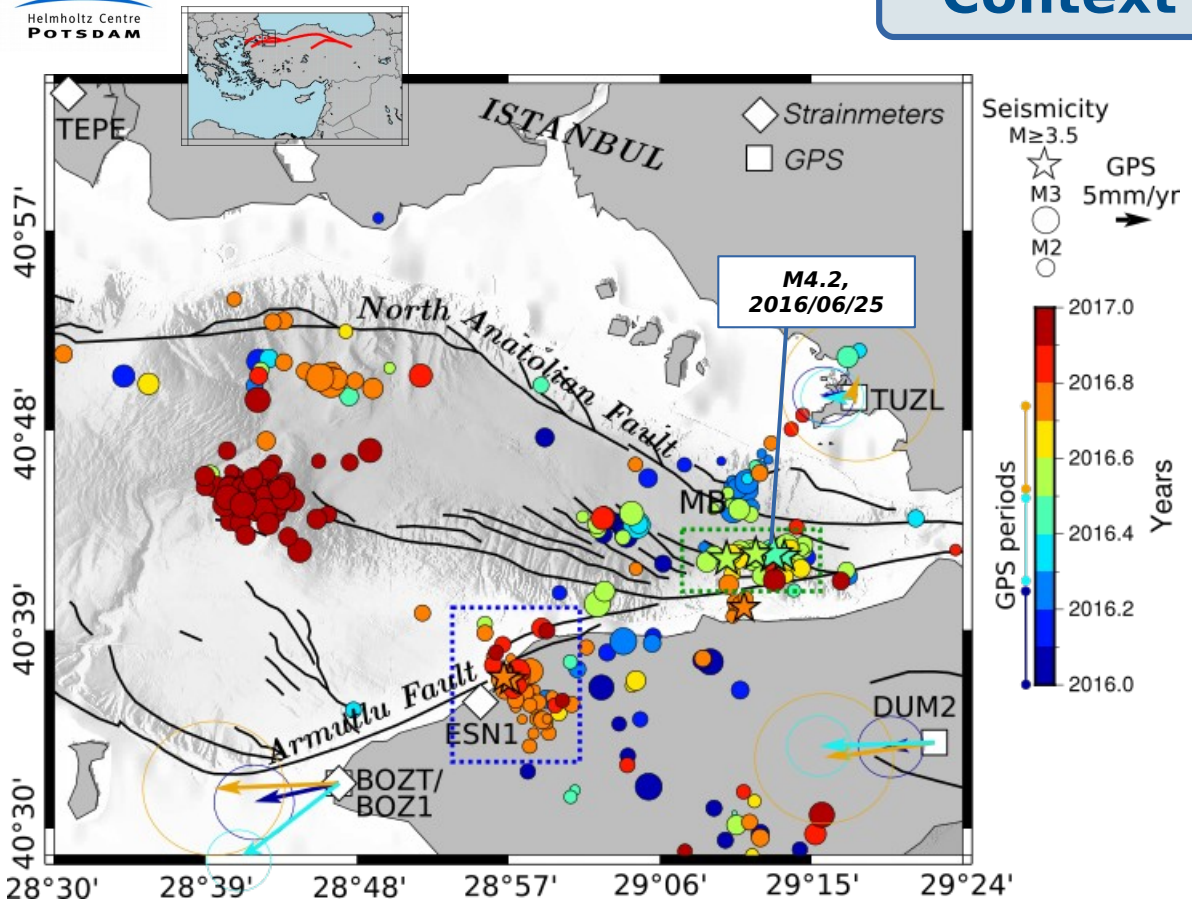

Location map: *seismic activity during 2016, location of the GPS and strainmeter stations, GPS velocities averaged on 3month-periods from Jan. to Sep. 2016. The colors indicate the time. The blue and green dashed boxes outline the seismicity clusters of the « Integration of the different data » part.*

The North Anatolian Fault (NAF) is a strike slip fault that runs from Eastern to Western Turkey. During the 20th century, more than 1000km have been ruptured in a sequence of M>7 earthquakes propagating from East to west between 1939 and 1999. The last portion that did not rupture during this sequence is the one located in the Marmara Sea, South of Istanbul.
In this study, we focus on the Eastern region of the Sea of Marmara, where the NAF is dividing in 3 sub-branches : the Main fault (NAF) north, a Middle Branch, and a Southern branch, that we will call « Armutlu Fault ». This portion of the NAF may constitute a significant hazard for the region, but it is challenging due to the off-shore nature of the faults.

Possible slow transients have been reported in the Eastern Sea of Marmara :

- Repeating events have been found before a M4.2 earthquake in June 2016, suggesting that some aseismic slip took place before this earthquake *(Malin et al. 2018)*
- A transient signal has been observed at ESN1 strainmeter station mid-2016 *(Martinez-Garzon et al. 2019)*

This transient signal being observed on a single station, its origin could not be well constrained.

In this study, we combine **strainmeter data from 2 stations** with **GPS** and **seismicity data** to understand better the origin of this transient signal. We apply a **vbICA technique** to remove the seasonal variations from the strainmeter signals, and we perform **Coulomb modelling** to constrain the geometry and location of the fault(s) at the origin of the observed transient signal.

GPS data

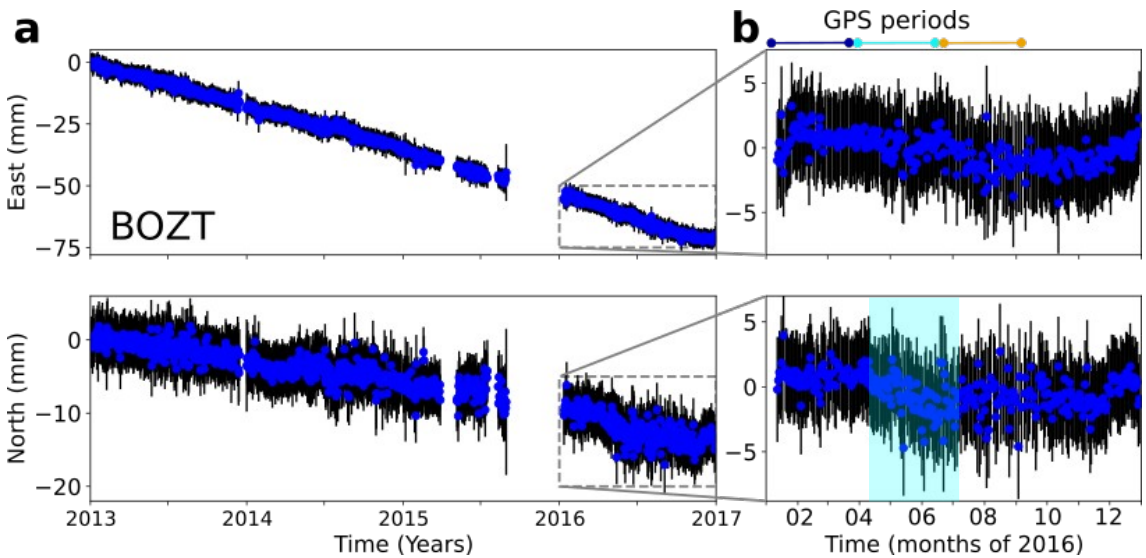

Figure1: *a) Signal recorded between 2013 and 2017, corrected from seasonal variations. The slope represents the long-term trend (~18mm/year). b) Zoom on 2016, signal corrected from seasonal variations, long-term trend removed. (Processed signals : courtesy of S.Ergintav, KOERI)*

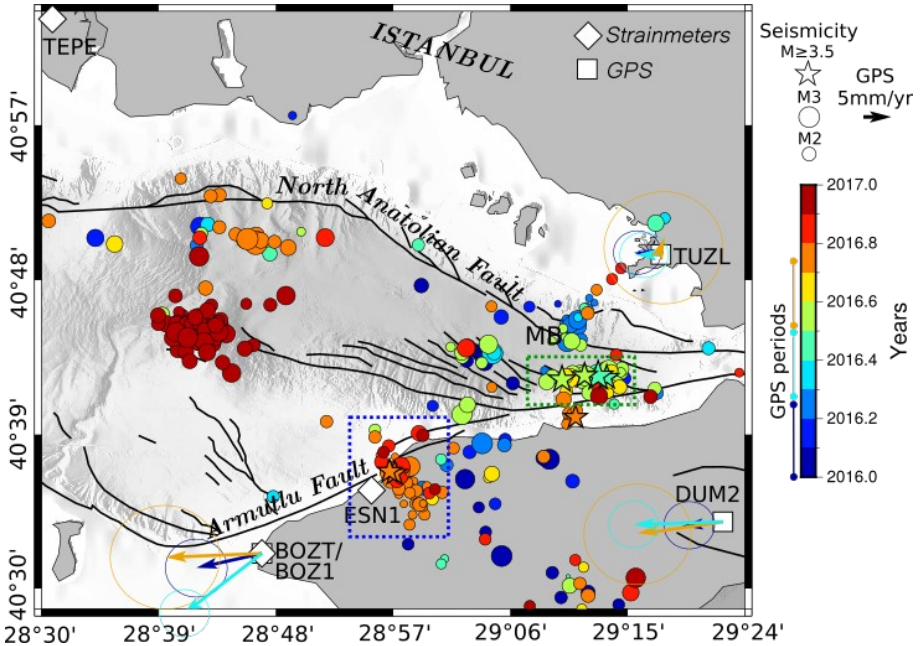

Figure2: *Location map (See « Context »). The GPS velocities (arrows) are color-coded with time.*

We corrected the GPS time series from seasonal variations and long-term trend estimated from a Trajectory Model *(Bevis & Brown 2014)*. An acceleration towards south of the displacement recorded at BOZT station is visible between April and July 2016 (Fig.1). The cumulative displacement on these 3 months is ~ 2mm. Fig.2 shows the decomposition of the velocities on 3-month periods at 3 GPS stations (BOZT, DUM2 and TUZL). TUZL and DUM2 stations do not show any significant change on the 3 periods, whereas BOZT station shows an increase of the velocity towards South during the light blue period (i.e. from April to July 2016). The direction of the transient signal recorded at BOZT is coherent with an acceleration of the slip along the Armutlu fault, with a combination of strike-slip and normal motion, consistent with the tectonic setting of the region.

Strainmeter data

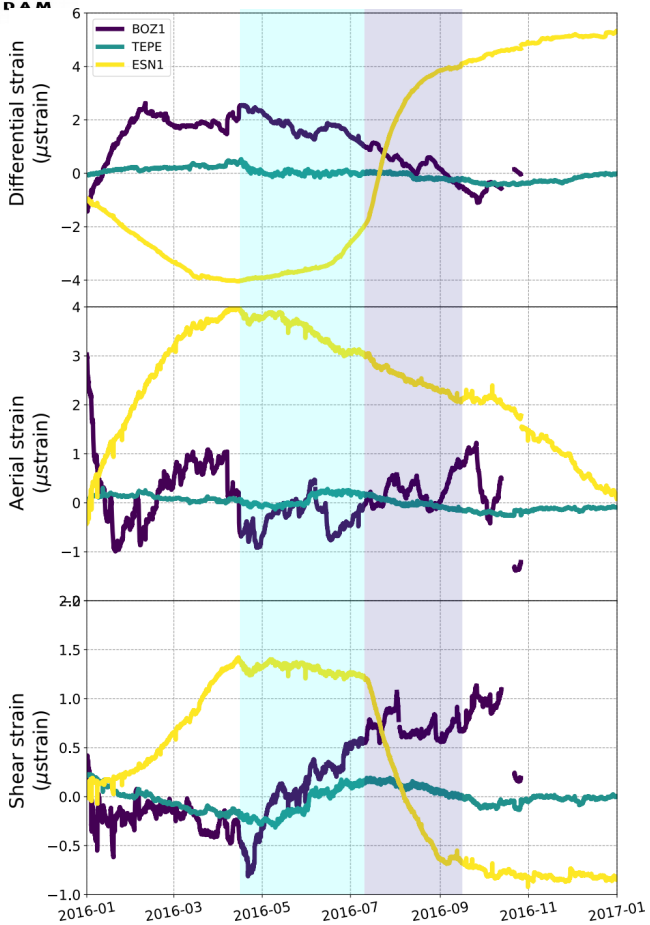

Figure1: *Strainmeter signals corrected from offsets, tides and borehole trend (Hodgkinson et al., 2013) and from seasonal variations (vbICA). The shaded areas highlight the 2 transients, that are mainly visible on BOZ1 and ESN1 stations on the differential and shear components..*

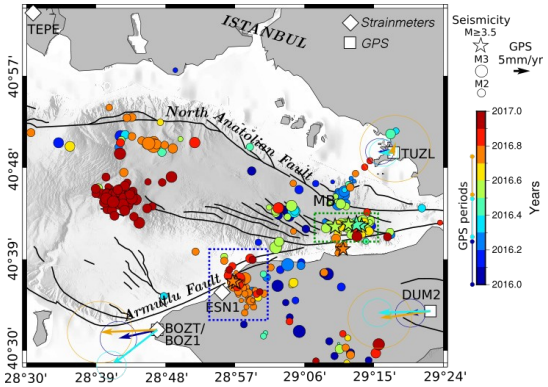

Figure2: *Location map. TEPE is located on the Northern coast, BOZ1 and ESN1 on the Southern coast.*

We use the 3 strainmeter stations that were working from 2016 to 2019. We correct them from offsets, tides and borehole trend *(Hodgkinson et al. 2013)*, and we apply a vbICA decomposition *(Gualandi et al. 2016)* to extract and remove the seasonal variations from the signals.

The TEPE station being dominated by the seasonal variations, we analyze only the temporal evolution of the signals recorded at stations BOZ1 and ESN1, which are also closer to the area of interest, considering the location of the seismicity.

We highlight **2 strain transients** in BOZ1 and ESN1 time series:

- A first one from **April to July 2016** (light blue area on Fig.1). This transient is mainly visible on station BOZ1, on the differential and shear components.
- A second one from **July to September 2016** (dark blue area on Fig.1), is clearly seen on ESN1 station, with a sharp change in the trend.

Both transients have an opposite sign on the two stations, **suggesting that the source is located in between**, potentially on the Armutlu fault. The change in amplitude evokes a **migration from West to East**.

Strainmeter data – vbICA method

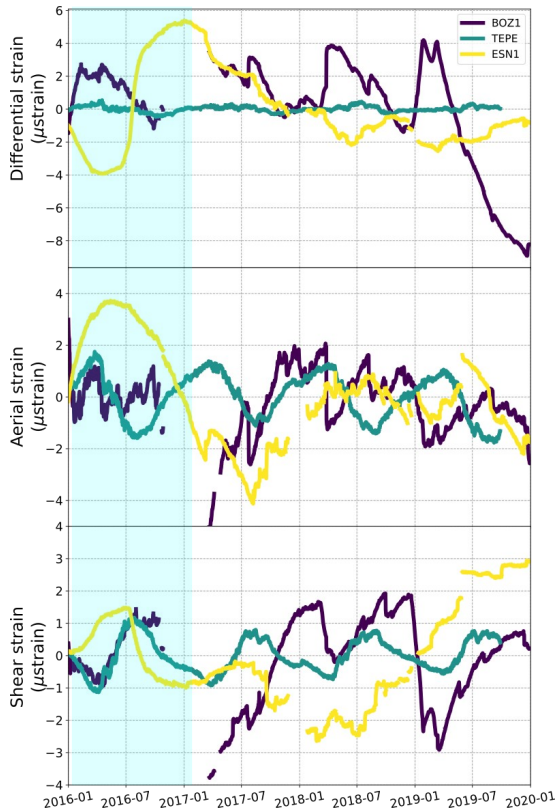

Figure1: *Strainmeter signals corrected from offsets, tides and borehole trend (Hodgkinson et al., 2013). The light blue area highlights the period where GPS data are available*

We use the 3 strainmeter stations that were working from 2016 to 2019, and we apply a vbICA decomposition *(Gualandi et al. 2016)* to extract and remove the seasonal variations from the signals.

The method in brief :

- Multivariate statistic approach
- We use a matrix X built with the data:
  T = number of epochs
  M = number of time series

$$\begin{pmatrix} X_{11} \cdots\cdots X_{1T} \\ \vdots \quad \ddots \quad \vdots \\ X_{M1} \cdots\cdots X_{MT} \end{pmatrix}$$

BOZ1 Differential strain
BOZ1 Aerial strain
BOZ1 shear strain
...
TEPE Shear strain

- Data **X** = a mix of a reduced number of sources (postseismic, seasonal,...)

$$\mathbf{X} = \mathbf{A\Sigma} + \mathbf{N}$$

with
- **A** = weights to mix sources
- **Σ** = Sources
- **N** = Gaussian noise

Hypotheses:

- Statistical independence of the sources
- Linear mix of the sources

Output :

Temporal and spatial evolution of the sources that generated the signal

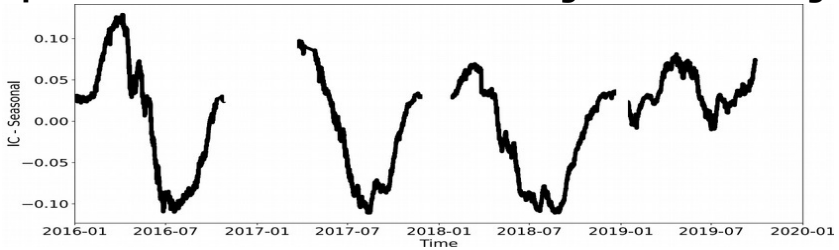

Figure2: *Seasonal component extracted using the vbICA decomposition*

Strainmeter data – vbICA result

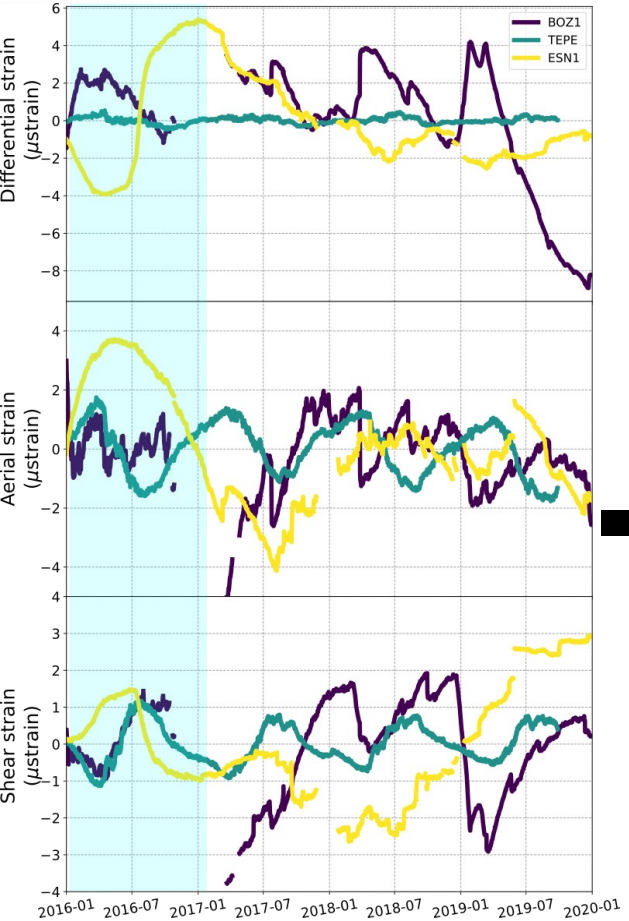

- After correcting for seasonal signal, TEPE station does not show any transient ⇒ we do not use this station for our analysis
- On the contrary, BOZ1 and ESN1 stations are only slightly affected by the seasonal variations
- The seasonal variations correlate with the temperature and pressure variations

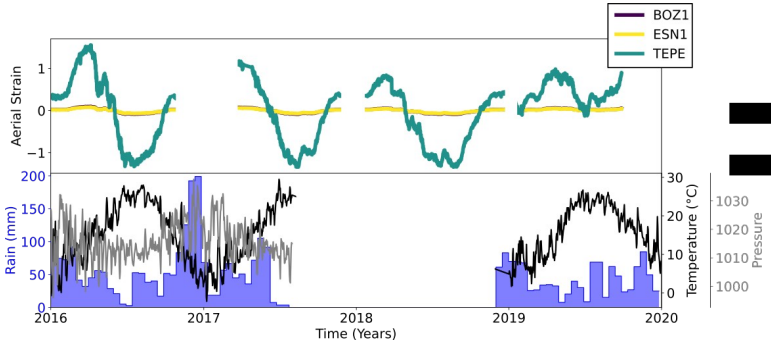

Figure2: *Comparison of the aerial strain reconstructed using only the extracted seasonal component at the 3 stations with meteorological data*

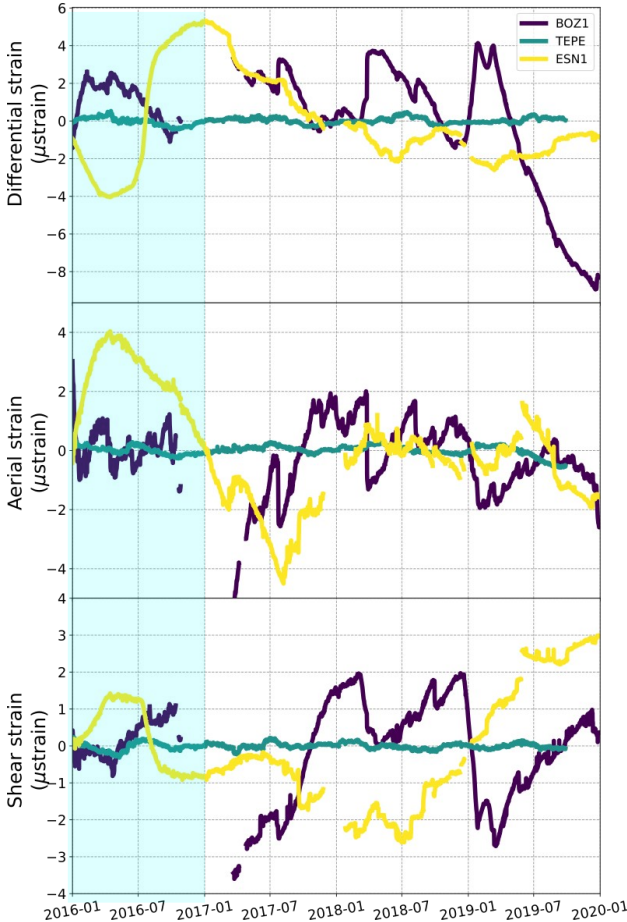

Figure1: *Strainmeter signals corrected from offsets, tides and borehole trend (Hodgkinson et al., 2013). The light blue area highlights the period where GPS data are available*

Figure3: *Strainmeter signals after removing the seasonal variations extracted using a vbICA decomposition technique*

Integration of the different data

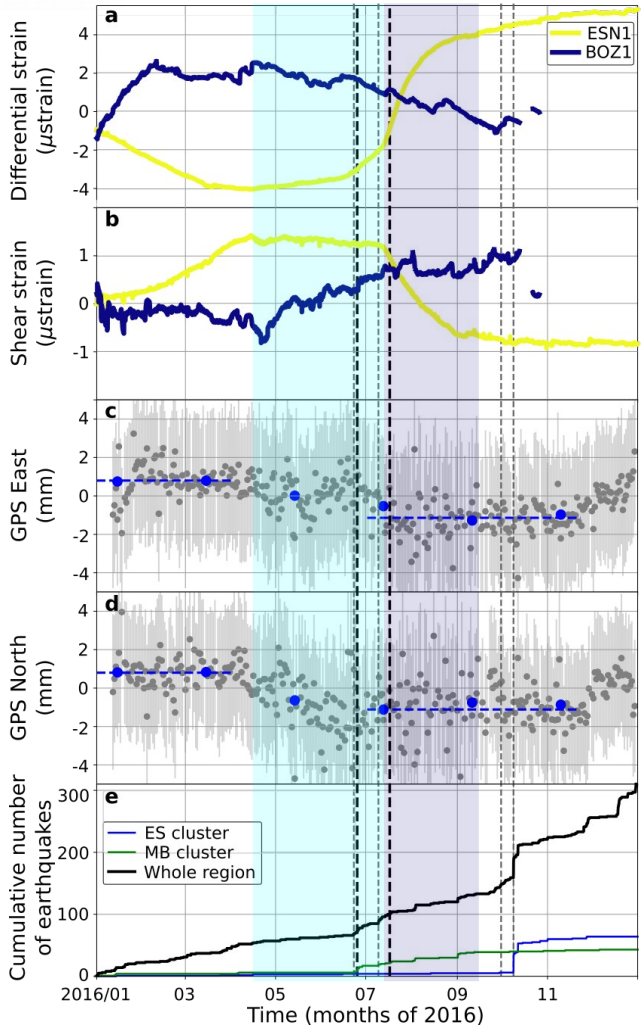

Figure1: *a) and b) Strainmeter signals corrected from offsets, tides and borehole trend and from seasonal variations (vbICA). c) and d) BOZT GPS signal corrected from seasonal variations, long-term trend removed. (Processed signals : courtesy of S.Ergintav, KOERI). e) Temporal evolution of the seismicity in the whole region (black curve), and on the two clusters highlighted in Fig.2 (green and blue curves). The vertical gray and black dashed lines indicate the occurrrence in the region of M>3.5 and M>4 earthquakes, respectively.*

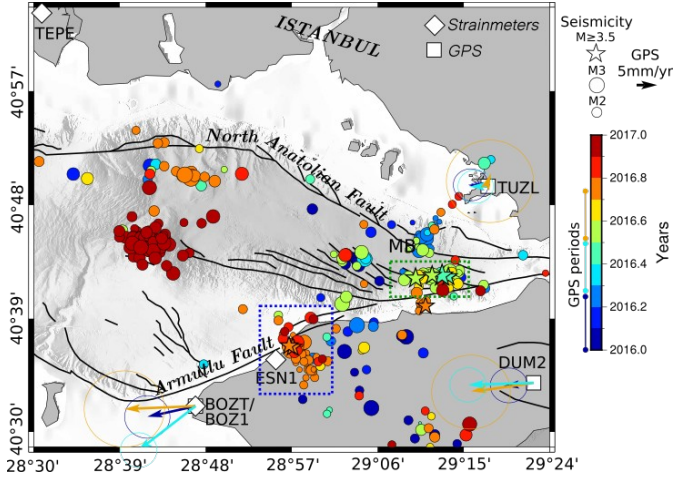

Figure2: *Location map. The blue and green dashed boxes highlight the clusters shown in Fig.1. The colored arrows show GPS velocities averaged on 3month-periods from Jan. to Sep. 2016.The colors indicate the time.*

The first **strain transient** (highlighted in light blue on Fig.1), recorded at both strainmeter stations, is **concomittent with the transient signal highlighted at the colocated GPS station BOZT**.
The second part of the signal (highlighted in dark blue on Fig.1) observed on the strainmeters is not recorded by the GPS. This, in addition to the fact that this second signal has an amplitude more than four times larger at ESN1 than at BOZ1, suggests that **the cause of this second signal is located close to ESN1 station.**

During the large signal recorded at ESN1 station in June-July 2016, a M3.5-M4 earthquake sequence occurred 30 km east, on the Middle Branch (highlighted by the green box on Fig.2). However, we do not observe changes in the strain signal trend concomittent with the different earthquakes of this sequence.

A few weeks after the end of the strain transients, the seismic cluster located close to ESN1 station (blue box on Fig.2) is showing the highest seismic activity in the region in 2016 (blue line in Fig.1e), suggesting that this **seismic activity has been inhanced by the previous transients**.

Coulomb Modelling

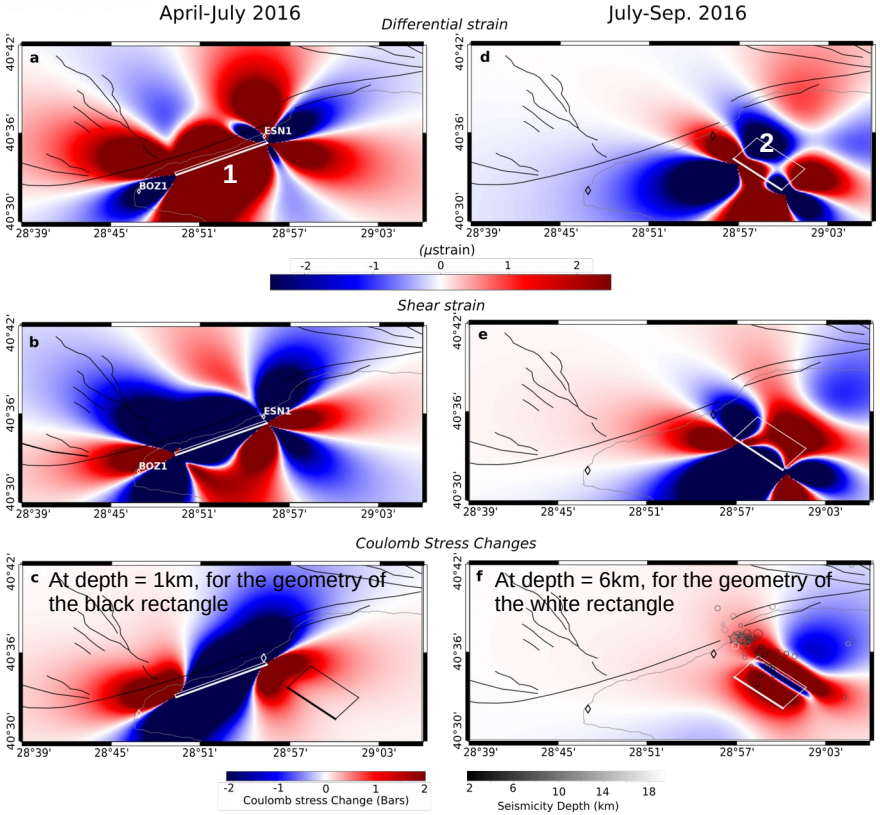

Figure1: *a,b,c) Forward modelling of the first transient. d,e,f) Forward modelling of the second transient. The diamonds note the station locations, the rectangles the geometries of the faults used to model the transients. c) ΔCFF generated by the white rectangular fault on receiver faults oriented as the black rectangular fault. f) ΔCFF generated by the white rectangular fault on on receiver faults oriented as the fault itself, i.e. as the seismicity that got activated at the end of the transient signal. The circles represent the seismicity occurring in October 2016.*

Parameters of the modelled faults :

1*. Strike=244°*
Dip = 80°
Rake = -150°
Top depth = 0km
L = 9.5km
W = 2km

2*. Strike=309°*
Dip = 55°
Rake = -90°
Top depth = 0km
L = 6km
W = 6km

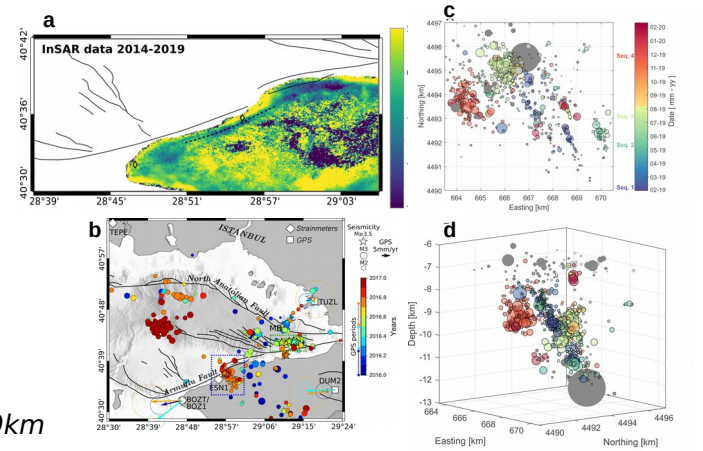

Figure2: *a) Velocity map derived from InSAR data from 2014-2019. b) Seismic activity during 2016. c and d) Map view and profile of the seismicity occurring in 2019 in the blue box defined in panel b. Seismicity detected and located using the temporary SMARTNET network (Martinez-Garzon et al., in review, SRL)*

We perform a forward modelling using *Okada (1992)* elastic dislocations to better constrain the location of the two transients.
The strain and GPS variations due to the first event (April to July 2016) can be reproduced at both stations by simulating a M5.5 event occurring between 0 and 2km depth **on an onshore fault between the two stations** (Fault 1 on Fig.1). The geometry of this fault has been infered from the InSAR data of Fig.2a.
The strain variation linked to the second event (July to Sptember 2016) can be reproduced by a M5.5 event occurring between 0 and 6km depth **on a perpendicular normal fault close to ESN1 station** (Fault 2 on Fig.1) This fault has been defined using the seismic activity recorded by a temporary network (Fig.2c & d). Fig.1c shows that the first transient has increased the stresses on the perpendicular fault, suggesting that **the first transient triggered the second one.**
The second transient has increased the stresses at the location of the seismic cluster activated in October 2016 (blue rectangle on Fig.2b), suggesting that **this second transient triggered the seismicity.**

Conclusions

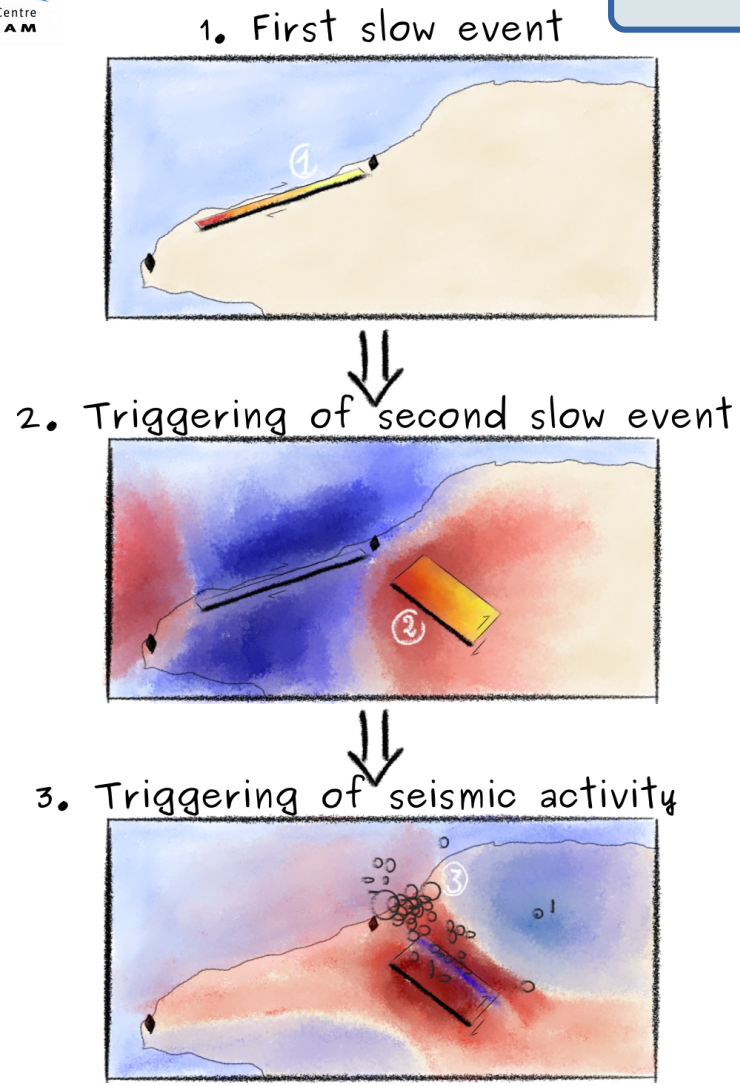

The detailed analysis of **strainmeter, GPS and seismicity data** allowed us to highlight the occurrence of **two successive slow events on perpendicular faults**. The first event occurs on a mainly strike-slip right-lateral fault that is little active seismically during the last 10 years. The second event occurs **on a pure normal fault,** that is activated by swarms during the last years. The first event, by changing the stress state on the perpendicular normal fault, triggered the second slow event. This slow shallow event, in turn, changed the stress state in the surrounding, and triggered the largest increase of seismicity in the region during the year 2016, activating the deepest part of the normal fault (between 4 and 10km). This activation initiated with two earthquakes of M>3.5 in two hours.

We present in this study forward models that are supporting our hypothesis. To perform an inversion for the slip distribution on these two faults, we need either more GPS and strainmeter stations or/and the capability to reliably extract transient signal from noisy InSAR time series. We cannot neither determine if the slip on the first fault continues to propagate eastward, because of the lack of stations in the region.

This study shows the **importance of combining different type of deformation data and seismicity data** to **analyze and understand the distribution of seismic and aseismic slip and their interactions**, in particular in a seismic region moderately active.